

# Diffractive Dijet Production and Nuclear Shadowing in $pA$ Interactions

S.E. Vance and D. Kharzeev <sup>a \*</sup>

<sup>a</sup>Physics Department, Brookhaven National Laboratory, Upton, NY 11973

We study the implications of non-universality observed recently in  $ep$  and  $\bar{p}p$  diffraction for nuclear shadowing and diffractive dijet production in  $pA$  collisions.

## 1. Nuclear Shadowing

Recently, measurements of diffractive jet rates in  $\bar{p}p$  interactions at the Tevatron were observed to be significantly lower than the theoretical expectations (for a review see [1]). The expectations were obtained using parameterizations of diffractive parton distribution functions extracted from  $ep$  interactions at HERA. The discrepancy between the data and the calculations revealed the breakdown of factorization or the onset of absorptive corrections in  $\bar{p}p$  diffractive events[2].

The physical reason for the breakdown of factorization is likely to be related to the different color structure of the probes in  $\bar{p}p$  and  $ep$  reactions. In  $ep$ , the compact, color singlet  $\bar{q}q$  pair produced by the virtual photon has a smaller probability of interacting with the external color fields and therefore has a larger rapidity gap survival probability. In  $\bar{p}p$ , the color octet gluon at comparable virtualities still interacts strongly with the external color fields, reducing its rapidity gap survival probability. The implications of the breakdown of factorization are now studied in nuclear shadowing and dijet production.

Nuclear shadowing is defined as the ratio of the  $pA$  to the  $pp$  total cross section,  $R = \sigma_{pA}/A\sigma_{pp}$ . The total cross section for  $pA$  interactions can be written as the sum of two terms

$$\sigma_{pA} \simeq A\sigma_{pN} - \delta\sigma_{pA}, \quad (1)$$

where the second term, representing elastic and inelastic [3] shadowing, can be written as[3,4]

$$\begin{aligned} \delta\sigma_{pA} \simeq & -8\pi \int d^2b \int_{-\infty}^{\infty} dz_1 \int_{z_1}^{\infty} dz_2 \rho_A(\vec{b}, z_1)\rho_A(\vec{b}, z_2) \\ & \times \int_{M_0^2}^{0.1s} dM^2 \cos((z_1 - z_2)/\lambda) \left. \frac{d^2\sigma_{pN}^{sd}}{dM^2 dt} \right|_{t \approx 0} \exp \left[ -\frac{\sigma_{XN}}{2} \int_{z_1}^{z_2} dz \rho_A(\vec{b}, z) \right], \end{aligned} \quad (2)$$

where  $d^2\sigma_{pN}^{sd}/dM^2 dt$  is the single diffractive cross section,  $\lambda = m_p(M^2 - m_p^2)/s$  is the coherence length of the resonance state X, and  $\rho_A(\vec{r})$  is the nuclear density ( $\rho_A$  is normalized to  $A$  and is taken to be Gaussian in all calculations presented here). In Eq. 2,

---

\*We would like to thank A. Capella, B. Kopeliovich and K. Goulianos for their comments. This manuscript was authored under Contract No. DE-AC02-98CH10886 with the U. S. Department of Energy.

$\delta\sigma$  depends upon the  $pp$  diffractive cross section. Unlike  $\gamma^*A$  interactions,  $R$  can not be directly associated with the shadowing of the structure functions (for a review see [5]).

In Regge theory, the dominant contribution to the single diffractive cross section at high energy is the triple Pomeron term. The single diffractive cross section can be expressed as

$$\frac{d^2\sigma^{sd}}{d(M^2/s)dt} = f_{P/p}(M^2/s, t)\sigma_T^{Pp}(M^2/s_0), \quad (3)$$

where  $f_{P/p}(M^2/s, t) = \frac{\beta_{Ppp}^2(t)}{16\pi} \left(\frac{M^2}{s}\right)^{1-2\alpha_P(t)}$  and  $\sigma_T^{Pp}(M^2/s_0) = \beta_{Ppp}(0)g(t) \left(\frac{M^2}{s_0}\right)^{\alpha_P(0)-1}$ . In these expressions,  $\beta_{Ppp}(t)$  represents the coupling of the Pomeron to the proton,  $s_0 = 1$  GeV, and the Pomeron intercept  $\alpha_P(t) = \alpha(0) + \alpha't = 1 + \epsilon + 0.25t$ , where  $\epsilon \sim 0.08 - 0.10$ . While this form is able to describe the diffractive  $ep$  cross section, it fails to describe the recently observed energy dependence of the diffractive  $\bar{p}p$  cross section.

A reasonable parameterization of the diffractive  $\bar{p}p$  cross section is obtained by normalizing  $f_{P/p}(M^2/s, t)$  according to the following scheme[6],

$$f_N(M^2/s, t) = \begin{cases} f_{P/p}(M^2/s, t) & \text{if } N(s) < 1 \\ \frac{1}{N(s)}f_{P/p}(M^2/s, t) & \text{if } N(s) > 1 \end{cases} \quad (4)$$

where  $N(s) = \int_{1.5/s}^{0.1} d(M^2/s) \int_{-\infty}^0 dt f_{P/p}(M^2/s, t)$ . In this scheme, the cross section becomes constant at high energies,  $\lim_{s \rightarrow \infty} \sigma_{sd}^N(s) = \text{constant}$ .

The effect of using this parameterization on the correction term in Eq. 2 is shown in Figure 1. Here, the solid line is a calculation of  $\delta\sigma$  for  $A = 100$  with the parameterization, while the dashed line is the naïve triple Pomeron contribution. The normalization scheme needed to reproduce  $\bar{p}p$  data results in a dramatic reduction of the shadowing in  $pA$ .

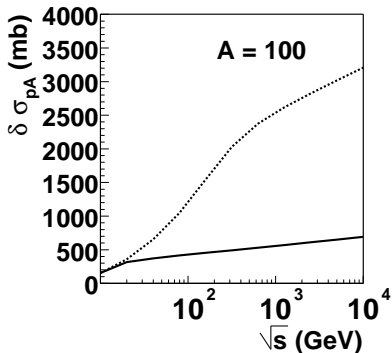


Figure 1. Calculations of the correction term,  $\delta\sigma_{pA}$ , for  $A = 100$  with (solid line) and without (dashed line) the normalization scheme of Eq. 4.

## 2. Diffractive dijet production

A simple formula for calculating diffractive dijet production will be utilized in this section. To begin, the hadronic state  $|h_l\rangle$  is expanded in terms of its diffractive eigenstates  $|\alpha\rangle$  [7,8],

$$|h_l\rangle = \sum_{\alpha} C_{l\alpha} |\alpha\rangle \quad (5)$$

The diffractive cross section can be expressed as the sum over the cross sections for all diffractive final states minus the elastic cross section,

$$\sigma_{pA}^{diff} = \sum_l \sigma(pA \rightarrow h_l A) - \sigma_{pA}^{el} \quad (6)$$

$$= \int d^2b \left[ \sum_l |C_{l\alpha}|^2 e^{-\sigma_{\alpha} T(\vec{b})} - \left( \sum_l |C_{l\alpha}|^2 e^{-\sigma_{\alpha} T(\vec{b})} \right)^2 \right], \quad (7)$$

where  $T(\vec{b}) = \int_{-\infty}^{\infty} dz \rho(\vec{b}, z)$  is the nuclear thickness function.

Assuming that  $|C_{l\alpha}|^2 = 1/2$ , the cross sections are related according to  $\sigma_{\alpha} = \sigma_{tot} \pm \Delta$ , where  $\Delta^2 = 16\pi \int dM^2 \frac{d\sigma}{dM^2 dt}$ , and the terms in Eq. 7 can then be written as

$$\sum_{\alpha} |C_{l\alpha}|^2 e^{\frac{1}{2}\sigma_{\alpha} T(\vec{b})} = \frac{1}{2} e^{\frac{1}{2}\sigma_{tot} T(\vec{b})} \left( e^{-\frac{1}{2}\Delta \tilde{T}^2(\vec{b}, M^2)} + e^{\frac{1}{2}\Delta \tilde{T}^2(\vec{b}, M^2)} \right), \quad (8)$$

where  $\tilde{T}(\vec{b}, M^2) = \int_{-\infty}^{\infty} dz \rho(\vec{b}, z) e^{iz/\lambda(s, M^2)}$ .

Substituting Eq. 8 into Eq. 7, the diffractive cross section can be expressed as

$$\sigma_{pA}^{diff} = 4\pi \int d^2b \int dM^2 \tilde{T}^2(\vec{b}, M^2) e^{-\sigma_{pp}^{tot} T(\vec{b})} \left. \frac{d\sigma_{pp}}{dM^2 dt} \right|_{t=0}, \quad (9)$$

and the ratio of the  $pA$  to  $pp$  differential diffractive cross section is

$$R(M^2) = \frac{d\sigma_{pA}^{diff}}{dM^2} \bigg/ A \frac{d\sigma_{pp}^{diff}}{dM^2} = \frac{4\pi}{A} \int d^2b \tilde{T}^2(\vec{b}, M^2) e^{-\sigma_{pp}^{tot} T(\vec{b})}. \quad (10)$$

At large  $M^2$ , Eq. 10 represents the ratio of the diffractive dijet production in  $pA$  to  $pp$ . In Figure 2,  $R(M^2)$  is plotted for  $A = 20$  (higher curve) and for  $A = 100$  (lower curve) at  $\sqrt{s} = 100$  GeV. As  $A$  increases, fewer diffractive dijets are produced relative to  $pp$ .

A similar formula applies for  $\gamma^*A$  diffractive dijet production (changing  $\frac{d\sigma_{pp}^{diff}}{dM^2} \rightarrow \frac{d\sigma_{\gamma^*p}^{diff}}{dM^2}$  and  $\sigma_{pp}^{tot} \rightarrow \sigma_{\gamma^*p}^{tot}$ ). The ratio for  $\gamma^*A$  is shown in Figure 3. The ratio of dijets with the  $\gamma^*$  probe is larger than in  $pA$ , since  $\sigma_{pp}^{tot} > \sigma_{q\bar{q}p}^{tot}$ .

Measurements of diffractive dijet production and nuclear shadowing in  $pA$  interactions at RHIC energies are needed to better understand the nature of diffraction and the quark-gluon wave function of the nucleus.

## REFERENCES

1. H. Abramowicz, Int. J. Mod. Phys. A15S1 (2000) 495 [hep-ph/0001054].

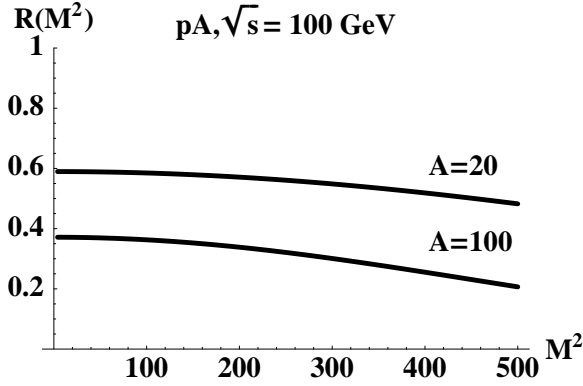


Figure 2. Calculations of the ratio,  $R(M^2)$ , of the diffractive cross sections of  $pA$  to  $pp$  are shown for  $A = 20$  and  $A = 100$  at  $\sqrt{s} = 100$  GeV.

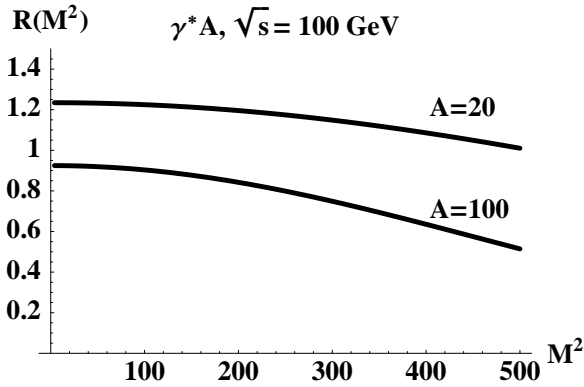


Figure 3. Calculations of the ratio,  $R(M^2)$ , of the diffractive cross sections of  $\gamma^*A$  to  $\gamma^*p$  are shown for  $A = 20$  and  $A = 100$  at  $\sqrt{s} = 100$  GeV.

2. J. C. Collins, Phys. Rev. D57 (1998) 3051 [hep-ph/9709499]; erratum Phys. Rev. D61, 2000 (1998).
3. V.N. Gribov, Sov. Phys. JETP 29 (1969) 483.
4. V.A. Karmanov and L.A. Kondratyuk, JETP Lett. 18 (1973) 266.
5. G. Piller and W. Weise, Phys. Rep. 330 (2000) 1; [hep-ph/9908230].
6. K. Goulianos and J. Montanha, Phys. Rev. D59 (1999) 114017; [hep-ph/9805496]; K. Goulianos, Phys Lett B358 (1995) 379; Erratum: ib. B363 (1995) 268.
7. P.G. Grassberger, Nucl. Phys. 125B (1977) 83.
8. H.I. Miettinen and J. Pumplin, Phys. Rev. 18D (1978) 1696.